

Hypervalent Ammonium Radicals. Effects of Alkyl Groups and Aromatic Substituents

Scott A. Shaffer, Martin Sadilek, and František Tureček*

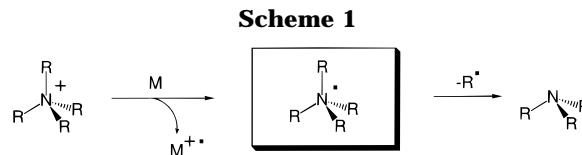
Department of Chemistry, Bagley Hall, Box 351700, University of Washington, Seattle, Washington 98195-1700

Received February 15, 1996[®]

Neutralization by collisional electron transfer of gaseous benzylalkylammonium ions produces transient hypervalent radicals whose dissociations depend on the substituents in the aromatic ring and at the amine nitrogen atom. Benzylammonium radical, $C_6H_5CH_2NH_3^+$, dissociates mainly by N–H bond cleavage to give benzylamine. Dissociation of the CH_2-N bond to benzyl radical and ammonia is less abundant. Benzylmethylammonium, $C_6H_5CH_2NH_2CH_3^+$, dissociates by CH_2-N , $N-CH_3$, and N–H bond cleavages to give methylamine, benzyl radical, benzylamine, and *N*-methylbenzylamine. Benzyltrimethylammonium, $C_6H_5CH_2N(CH_3)_3^+$, undergoes loss of dimethylamine and hydrogen, while the loss of methyl is less important. (2,3,4,5,6-Pentafluorobenzyl)-dimethylammonium radical, $C_6F_5CH_2N(CH_3)_2^+$, dissociates mainly by fission of the pentafluorophenyl ring to give C_nF_m fragments with CF^+ as the dominating product, while bond dissociations at the hypervalent nitrogen atom are less important. The relative stabilities of pentafluorobenzyl and tropylium cations and radicals are assessed by ab initio calculations. (3,5-Dinitrobenzyl)-dimethylammonium radical, $(NO_2)_2C_6H_3CH_2N(CH_3)_2^+$, undergoes competitive losses of hydrogen and NO and intramolecular proton transfer onto the dinitrophenyl ring. Mechanisms for these reactions are suggested involving dissociative electron attachment at the aromatic ring and formation of hypervalent ammonium radicals and zwitterionic intermediates.

Introduction

Hypervalent ammonium radicals are transient intermediates in one-electron reduction of ammonium ions in solution or the gas phase. Ammonium radicals, which are denoted as (9-N-4) according to Perkins et al.,¹ formally have nine valence electrons at the nitrogen atom and exhibit unusual electronic properties and reactivities.^{2,3} While undetectable in solution because of their instability,⁴ several hypervalent organic ammonium radicals have been generated in the gas phase by collisional reduction of their ammonium ion counterparts, and their dissociations have been studied by neutralization–reionization ($^+NR^+$) mass spectrometry, as reviewed.^{2b,5} Briefly, ammonium cations are prepared by protonation in the gas phase and accelerated to a kiloelectronvolt kinetic energy. The fast cations are allowed to collide with a thermal atomic or molecular target gas, which serves as an electron donor in a glancing collision. The cation–donor interaction time is typically $<10^{-14}$ s, which results in an essentially vertical electron transfer, such that the



nascent fast neutral species is formed with the geometry of the precursor ion. The residual ions are removed electrostatically, and the fast neutrals are analyzed by mass spectrometry following reionization to cations or anions.⁵ Collisional activation,⁶ unimolecular kinetics,⁷ photodissociation, and photoionization⁸ are some of the auxiliary methods that have been used to elucidate the energetics and electronic structure of the neutral intermediates.

Simple organic ammonium radicals, $CH_3ND_3^+$,^{2c,d} $(CH_3)_2ND_2^+$,⁹ and $(CD_2H)(CH_3)_2NH^+$,¹⁰ show metastability in the gas phase, such that intact species of microsecond lifetimes can be detected by mass spectrometry. Other organic ammonium radicals, e.g., $(CH_3)_4N^+$, $C_6H_5CH_2N(CH_3)_3^+$,¹¹ $n-C_7H_5NH(CH_3)_2^+$, and $(CH_3)_2N(CH_2)_nNH(CH_3)_2^+$ ¹² have been found to dissociate completely within a few microseconds following their formation in the gas phase. Aliphatic hypervalent ammonium radicals have been found to decompose by both N–C and N–H bond cleavages (Scheme 1), although the relative propensities for these dissociations depended on the system under study.^{9–12}

[®] Abstract published in *Advance ACS Abstracts*, July 15, 1996.

(1) Perkins, C. W.; Martin, J. C.; Arduengo, A. J.; Lau, W.; Alegria, A.; Kochi, J. K. *J. Am. Chem. Soc.* **1980**, *102*, 7753.

(2) (a) Gellene, G. I.; Cleary, D. A.; Porter, R. F. *J. Chem. Phys.* **1982**, *77*, 3471–3477. (b) Gellene, G. I.; Porter, R. F. *Acc. Chem. Res.* **1983**, *16*, 200–207. (c) Gellene, G. I.; Porter, R. F. *J. Phys. Chem.* **1984**, *88*, 6680–6684. (d) Jeon, S.-J.; Raksit, A. B.; Gellene, G. I.; Porter, R. F. *J. Am. Chem. Soc.* **1985**, *107*, 4129–4133.

(3) (a) McMaster, B. N.; Mrozek, J.; Smith, V. H. *Chem. Phys.* **1982**, *73*, 131. (b) Cardy, H.; Liotard, D.; Dargelos, A.; Poquet, E. *Chem. Phys.* **1983**, *77*, 287. (c) Kaspar, J.; Smith, V. H.; McMaster, B. N. *Chem. Phys.* **1985**, *96*, 81. (d) Kassab, E.; Evleth, E. M. *J. Am. Chem. Soc.* **1987**, *109*, 1653. (e) Boldyrev, A. I.; Simons, J. *J. Chem. Phys.* **1992**, *97*, 6621.

(4) Gedye, R. N.; Sadana, Y. N.; Eng, R. *J. Org. Chem.* **1980**, *45*, 3721.

(5) (a) Danis, P. O.; Wesdemiotis, C.; McLafferty, F. W. *J. Am. Chem. Soc.* **1983**, *105*, 7454. For recent reviews, see: (b) Holmes, J. L. *Mass Spectrom. Rev.* **1989**, *8*, 513. (c) McLafferty, F. W. *Science (Washington)* **1990**, *247*, 925. (d) McLafferty, F. W. *Int. J. Mass Spectrom. Ion Processes* **1992**, *118/119*, 221. (e) Turecek, F. *Org. Mass Spectrom.* **1992**, *27*, 1087. (f) Goldberg, N.; Schwarz, H. *Acc. Chem. Res.* **1994**, *27*, 347.

(6) Feng, R.; Wesdemiotis, C.; Baldwin, M. A.; McLafferty, F. W. *Int. J. Mass Spectrom. Ion Processes* **1988**, *86*, 95.

(7) (a) Kuhns, D. W.; Shaffer, S. A.; Tran, T. B.; Turecek, F. *J. Phys. Chem.* **1994**, *98*, 4845. (b) Kuhns, D. W.; Turecek, F. *Org. Mass Spectrom.* **1994**, *29*, 463.

(8) Sadilek, M.; Turecek, F. *J. Phys. Chem.* **1996**, *100*, 9610.

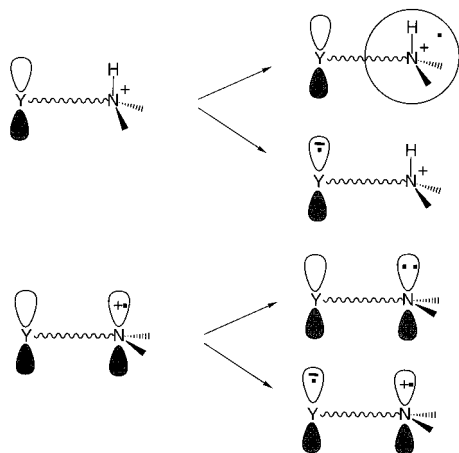
(9) Sadilek, M.; Nguyen, V. Q.; Turecek, F. *Chem. Phys. Lett.* submitted for publication.

(10) Shaffer, S. A.; Turecek, F. *J. Am. Chem. Soc.* **1994**, *116*, 8647.

(11) Beranova, S.; Wesdemiotis, C. *Int. J. Mass Spectrom. Ion Processes* **1994**, *134*, 83–102.

(12) Shaffer, S. A.; Turecek, F. *J. Am. Soc. Mass Spectrom.* **1995**, *6*, 1004.

Scheme 2



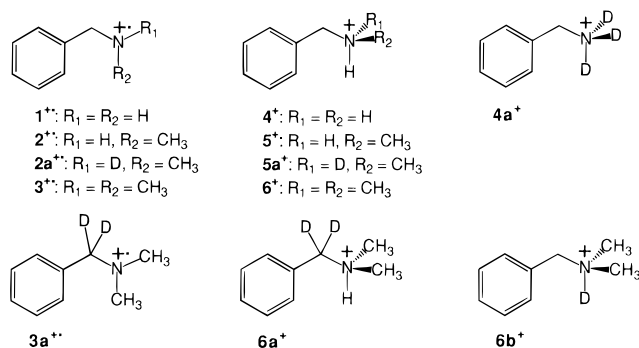
Ammonium radicals derived from simple monoamines have also been studied by theory.^{3,10} The odd electron is thought to be deposited into one of the diffuse orbitals centered at the amine group, where it typically causes a substantial weakening of one of the N–H bonds.^{3e,10} In contrast, N–CH₃ bond cleavages were predicted by theory to require substantial activation energies on the ground state potential energy surface which should prevent them from competing with N–H bond dissociations. To explain the occurrence of N–C bond cleavages, which were observed experimentally,^{9–12} formation of higher excited states in hypervalent onium radicals has been considered theoretically¹⁰ and recently confirmed experimentally.⁸

An interesting and qualitatively new possibility arises in fast reduction of larger bi- or polyfunctional ammonium ions that provide two or more distinct acceptor sites for electron capture (Scheme 2). Neutralization at the ammonium center can form a hypervalent radical in its ground or excited electronic states, in which fragmentations are likely to proceed by cleavages of bonds adjacent to the nitrogen atom.^{2,9–12} In contrast, electron capture by a manifold of unoccupied orbitals located at a distant atom or functional group will result in the formation of a zwitterion whose dissociations may be induced by the charge at either the cationic or anionic centers and thus lead to distinct products. Previous studies of simple zwitterions of the ⁻CH₂XH_n⁺ type indicated stability or metastability of some of these species on the microsecond time scale,¹³ while contradicting theoretical predictions.^{5b,14} However, dissociations of those simple systems involved mostly C–X bond cleavages.¹³

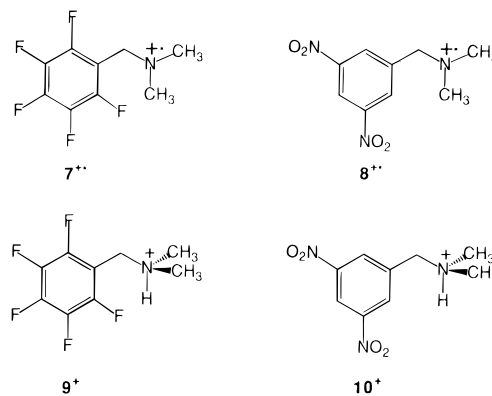
A similar mechanism for electron capture can be invoked for fast neutralization of bi- or polyfunctional amine cation radicals. In this case, the electron entering the semioccupied n-orbital at the nitrogen atom recreates the stable molecule in its ground electronic state, whereas electron capture by a distant unoccupied orbital results in the formation of an excited electronic state. The latter corresponds formally to an intramolecular charge-

transfer complex¹⁵ whose dissociations may be charge-induced as observed recently for photoexcited aromatic molecules in the gas phase.¹⁶ Another mechanism for de-excitation of charge-transfer complexes is photon emission, as observed for the interaction of anthracene anion radical with triphenylamine cation radical, which resulted in chemiluminescence.¹⁷

In this work we investigate the formation and dissociations of molecules and hypervalent radicals formed by fast collisional reduction of substituted benzylamine cation radicals **1**⁺–**3**⁺, **7**⁺, and **8**⁺ and ammonium ions **4**⁺–**6**⁺, **9**⁺, and **10**⁺. The latter cations allow one to find



ionization conditions under which the initial protonation site is localized at the amine nitrogen. The electron capture process can thus be investigated by analyzing the dissociations taking place at the ammonium center, in the aromatic ring, or in its substituents. The electronic properties of the aromatic systems are modified by introducing electron-withdrawing substituents (F and NO₂ in **7**, **9**⁺, and **8**, **10**⁺, respectively) that increase the electron affinity of the molecule through σ and π effects and thus possibly provide bound states at the aromatic ring for the incoming electron.¹⁸ Deuterium-labeled ions **2a**⁺, **3a**⁺, **4a**⁺, **6a**⁺, and **6b**⁺ are used to elucidate the dissociation mechanisms and detect proton-transfer rearrangements.



Experimental Section

Methods. Neutralization–reionization (⁺NR⁺, signifying neutralization of precursor cations and reionization of intermediate neutrals to form cations) spectra were obtained on a

(13) (a) Wesdemiotis, C.; Feng, R.; Danis, P. O.; Williams, E. R.; McLafferty, F. W. *J. Am. Chem. Soc.* **1986**, *108*, 5847. For the hitherto unsettled controversy about the stability of halogenated ylides, see: (b) Terlouw, J. K.; Kieskamp, W. M.; Holmes, J. L.; Momms, A. A.; Burgers, P. C. *Int. J. Mass Spectrom. Ion Processes* **1985**, *64*, 245. (c) Hop, C. E. C. A.; Bordas-Nagy, J.; Holmes, J. L.; Terlouw, J. K. *Org. Mass Spectrom.* **1988**, *23*, 155.

(14) (a) Pople, J. A.; Raghavachari, K.; Binkley, J. S.; Schleyer, P. v. R. *J. Am. Chem. Soc.* **1983**, *105*, 6389. (b) Yates, B. F.; Bouma, W. J.; Radom, L. *J. Am. Chem. Soc.* **1984**, *106*, 5805.

(15) Bender, C. J. *Chem. Soc. Rev.* **1986**, *15*, 475.

(16) (a) Chatorajj, M.; Laursen, S.; Paulson, B.; Chung, D. D.; Closs, G. L.; Levy, D. H. *J. Phys. Chem.* **1992**, *96*, 8778. (b) Chatorajj, M.; Chung, D. D.; Paulson, B.; Closs, G. L.; Levy, D. H. *J. Phys. Chem.* **1994**, *98*, 3361.

(17) Weller, A.; Zachariasse, K. *Chem. Phys. Lett.* **1971**, *10*, 590.

(18) (a) Dillow, G. W.; Kebarle, P. *J. Am. Chem. Soc.* **1989**, *111*, 5592. For a review see: (b) Kebarle, P.; Chowdhury, S. *Chem. Rev.* **1987**, *87*, 513.

tandem quadrupole acceleration-deceleration mass spectrometer described previously.¹⁹ Volatile samples were introduced into the ion source from a small glass reservoir maintained at 25 °C, and the sample intake was regulated by a Teflon needle valve to achieve pressures in the range of 8×10^{-6} to 2×10^{-5} Torr. Less volatile samples were introduced from a heated glass direct probe extending to the ion source. Precursor cation radicals were generated by electron impact ionization of the corresponding amines at 70 eV, emission current 500 μ A, ion source temperature 150 °C. Cations **4**⁺–**6**⁺, **9**⁺, and **10**⁺ were prepared by isobutane or ammonia chemical ionization (protonation with C₄H₉⁺ or NH₄⁺, respectively) of the amines in a tight ion source of our design. The chemical ionization conditions were as follows: emission current, 1 mA; electron energy, 100 eV; isobutane pressure, 2×10^{-4} Torr as read on the ionization gauge located outside the ion source. The reagent gas pressure and ion source potentials were adjusted to optimize protonation and minimize electron ionization of the amines such as to obtain ion abundance ratios of $[M + H]^+/[M^+] > 10$ for most ions. The deuterated ions **4a**⁺ and **6b**⁺ were prepared by protonation with ND₄⁺ and C₄D₉⁺ generated by chemical ionization (CI) of ND₃ (Cambridge Isotopes, 99% D) and (CD₃)₃CD (MSD Isotopes, 99% D), respectively. The ion source and gas inlet walls were conditioned with D₂O at 2×10^{-5} Torr for 1 h prior to the deuteration experiments. The precursor ions were passed through a quadrupole mass filter operated at low mass resolution, accelerated to 8200 eV, and neutralized by collisions with gaseous CH₃SSCH₃, (CH₃)₃N, or Xe at pressures such as to achieve 70% transmittance of the precursor ion beam. For the electrostatic potentials used, the precursor ion lifetimes are estimated at 40–58 μ s for m/z 106–226. The neutral products were separated by reflecting the remaining ions electrostatically and then reionized by collisions with oxygen at pressures such as to achieve 70% transmittance of the precursor ion beam. The intermediate neutral lifetimes were in the 4.9–7.2 μ s range for precursor ions of m/z 106–226. The reionized cations were decelerated by an electrostatic lens, filtered by kinetic energy, and mass-analyzed by a quadrupole mass filter, which was scanned in link with the deceleration voltage.^{19,20} Such linked scans achieve both product ion resolution depending on the tunable m/z bandwidth of mass analyzer, and precursor ion resolution depending on the fixed bandwidth of the kinetic energy filter and product/precursor mass ratio.²⁰ For example, linked-scan detection of the reionized ion at m/z 31 from **7**⁺ (m/z 225) achieves precursor mass resolution of 45, i.e., precursor ions within ± 2.5 mass units of m/z 225 can contribute to the peak intensity at m/z 31. Some contamination from the precursor-ion isotope satellites thus occurs, while product ions from precursors of $m/z < 222$ are filtered out.

The use of wide apertures in the collision cells (5 mm) and ion refocusing by the lens system²⁰ allow efficient collection of fragments scattered within 0.46° full angle. The reionized and mass-analyzed products are detected with essentially identical kinetic energies given by the voltage applied to the electron multiplier, thus minimizing discrimination effects.²¹ Collisionally activated dissociation (CAD) of the intermediate neutrals was carried out by admitting helium in the differentially pumped neutral drift region at a pressure such as to achieve 50% transmittance of the precursor ion beam. The drift region was floated at +250 V, so that any cations formed there had kiloelectronvolt kinetic energies upon exit, $T = (m_p/m_f)T_p + 250$ eV, where m_p and m_f are the precursor and product masses, respectively, and T_p is the precursor kinetic energy. These ions retain their kiloelectronvolt kinetic energies and are rejected by the energy filter. Hence, products of neutral CAD that are reionized in the reionization cell are

detected selectively.^{19,20} The reported spectra were averaged over 25–30 repetitive scans obtained at scan rates of 1 s (75 data points) per mass unit.

Collisionally activated dissociation (CAD) spectra of ions at 4 keV laboratory kinetic energy were taken on a Kratos Profile HV-4 double-focusing mass spectrometer equipped with a collision cell of our design that was mounted in the first field-free region and grounded. Oxygen was used as collision gas at 70% transmittance of the precursor ion beam. The spectra were obtained by scanning the magnet (B) and electrostatic (E) sectors while maintaining the B/E ratio constant (B/E-linked scan). The reported spectra are averages of at least six repetitive scans obtained at dynamic mass resolution >500.

Materials. Benzylamine, *N*-methylbenzylamine, and *N,N*-dimethylbenzylamine were purchased from Aldrich and used as received. *N,N*-Dimethyl(benzyl-*d*₂)amine (**3a**) was prepared by LiAlD₄ (Aldrich, 99% D) reduction of *N,N*-dimethylbenzamide in tetrahydrofuran and characterized by its 70 eV EI mass spectrum: m/z (rel intensity) 138 (5), 137(M⁺, 46), 136 (6.5), 135 (18), 121 (2), 120 (3), 120 (1), 118 (1.5), 94 (9), 93 (47), 92 (4), 91 (5), 79 (1), 78 (1), 77 (2), 69 (2), 67 (7), 66 (5), 65 (3), 64 (2), 63 (2), 61 (4), 60 (100), 59 (4), 58 (3), 53 (1), 52 (1.5), 51 (3), 50 (1), 45 (1.5), 44 (17), 43 (10), 42 (7), 41 (3), 40 (6), 39 (3).

***N*-Methylbenzylamine-*N-d*₁ (**2a**).** *N*-Methylbenzylamine 1.65 g, 13.6 mmol was added to a solution of D₃PO₄ prepared from 20 mL of D₂O and 1.6 g of P₂O₅. The homogeneous solution was stirred at 50 °C, and the deuterium oxide was distilled off at 50 Torr. The exchange was repeated with a fresh 20 mL portion of D₃PO₄. The solution was neutralized with 20 mL of 4 M NaOD in D₂O, the product was extracted in CH₂Cl₂ and dried, and the solution was taken down on a rotary evaporator. The 70 eV mass spectrum of the product, measured after having conditioned the ion source with D₂O vapor, showed 98% d₁ content. Mass spectrum: m/z (rel intensity) 123 (2.7), 122 (M-d₁⁺, 39), 121 (M-H, 100), 120 (5.2), 119 (2.3), 118 (1.3). Some back-exchange takes place in an untreated ion source.

***N,N*-Dimethyl-2,3,4,5,6-pentafluorobenzylamine (**7**).** A solution of 2,3,4,5,6-pentafluorobenzyl bromide (Aldrich, 5 g, 19 mmol) in 45 mL of CH₂Cl₂ was added drop-wise to 75 mL of CH₂Cl₂ solution saturated with anhydrous dimethylamine (2.38 g, 52 mmol) at 0 °C. After 4 h of stirring, TLC analysis (silica gel, elution with ethyl acetate/methanol 10:1) showed that the reaction was complete. The mixture was diluted with 50 mL of CH₂Cl₂, washed with 4 \times 30 mL of 10% aqueous potassium carbonate, and dried with anhydrous potassium carbonate. The solvent was distilled off, and the product was distilled at 76 °C/30 Torr to give 2.37 g (55%) of **7**. ¹H NMR (CDCl₃): 2.30 (s, 6H), 3.67 (m, 2H). Mass spectrum: m/z (rel intensity) 226 (1), 225 (M⁺, 13), 224 (8), 208 (1), 181 (33), 163 (1.5), 161 (3.5), 135 (1), 117 (2), 93 (4), 91 (4), 81 (2), 69 (2), 59 (3), 58 (100), 51 (2), 44 (4), 43 (28.5), 42 (33), 41 (3), 31 (3), 30 (2).

***N,N*-Dimethyl-3,5-dinitrobenzylamine (**8**).** A solution of 3,5-dinitrobenzyl chloride (Aldrich, 4 g, 18.5 mmol) in 75 mL of CH₂Cl₂ was added drop-wise to liquid anhydrous dimethylamine (190 mmol) at 0 °C. The mixture was stirred for 1 h, diluted with 25 mL of CH₂Cl₂, washed with water and 5% NaHCO₃, and dried with Na₂SO₄, and the solvent was distilled off in vacuo. The yellow-brown residue was dissolved in 50 mL of ether and triturated with hexane at 0 °C. The solid (mostly hydrochloride salts) was filtered off, and the solution was taken down on a rotary evaporator to give a bright-yellow oil that solidified on standing at 0 °C. Yield: 2.68 g (64%), single spot by TLC (Silica gel, ethyl acetate). ¹H NMR (CDCl₃): 8.94 (s, 1H), 8.55 (s, 2H), 3.64 (s, 2H), 2.31 (s, 6H). Mass spectrum: m/z (rel intensity) 226 (8), 225 (M⁺, 66), 224 (40), 208 (3), 181 (22), 178 (15), 135 (10), 133 (2), 132 (34), 90 (9), 89 (46), 77 (12), 76 (6), 75 (16), 74 (10), 63 (66), 62 (22), 59 (44), 58 (42), 57 (15), 51 (18), 50 (14), 46 (11), 45 (5), 44 (43), 43 (31), 42 (100), 41 (16), 39 (41), 30 (82), 29 (13), 27 (7), 15 (21). Amine **8** decomposed to non-volatile products

(19) Turecek, F.; Gu, M.; Shaffer, S. A. *J. Am. Soc. Mass Spectrom.* **1992**, *3*, 493.

(20) Shaffer, S. A.; Turecek, F.; Cerny, R. L. *J. Am. Chem. Soc.* **1993**, *115*, 12117.

(21) (a) Potter, W. E.; Mauersberger, K. *Rev. Sci. Instrum.* **1972**, *43*, 1327. (b) Kurz, E. A. *Am. Lab.* **1979**, *11*, 67–82. (c) la Lau, C. In *Topics in Organic Mass Spectrometry*, Adv. Anal. Instrum. Meth. Vol. 8; Burlingame, A. L., Ed.; Wiley: New York, 1970.

when heated in the ion source,²² so that only about 10 scans could be taken before the vapor pressure dropped below a few μ Torr, causing poorer signal-to-noise ratios in the $^+NR^+$ spectra of $\mathbf{8}^{3+}$ and $\mathbf{10}^+$ when compared with those of ions derived from chemically stable amine precursors.

Calculations. Standard ab initio calculations of the 2,3,4,5,6-pentafluorobenzyl and 1,2,3,4,5-pentafluorotropylium cations and radicals were carried out using the Gaussian 92 program.²³ Equilibrium geometries were optimized with the 3-21G basis set that was also used to obtain harmonic vibrational frequencies, which were scaled by 0.9 to calculate zero-point vibrational energies. The optimized geometries and vibrational frequencies are available as supporting information. The optimized 3-21G geometries were used for single-point energy calculations with the 6-31G(d) basis set. The size of these systems (344 primitive Gaussians for the 6-31G(d) basis set) precluded higher-level post-Hartree-Fock calculations that would presumably provide more accurate estimates for the relative stabilities of the cations and radicals under study.

Results

Hypervalent ammonium radicals formed by neutralization of ammonium ions can dissociate by C–N and N–H bond cleavages to form stable molecules and the complementary radicals, which are identified by mass spectrometry.^{2,9–12} In $^+NR^+$ experiments, products of neutral dissociations must be reionized to be detected, which introduces some overlap with the products of ion dissociations induced by the reionizing collisions. Hence, the products of ion dissociations must be known to distinguish both types of processes. Cation radicals corresponding to reionized molecules and cations corresponding to reionized radicals were therefore investigated through their collisionally activated dissociation (CAD) spectra to identify the major products of ion dissociations. $^+NR^+$ spectra of cation radicals were also investigated for signature ions that could be used to identify the molecules formed by dissociations of hypervalent ammonium radicals.

Collisionally Activated Dissociation and Neutralization of Cation Radicals. Electron ionization of the benzylamines under study forms stable cation radicals that give rise to abundant peaks in the corresponding mass spectra.²⁴ Ion dissociations of mass-selected molecular ions of $\mathbf{1}^{3+}$ – $\mathbf{3}^{3+}$ showed mostly simple bond cleavages giving rise to stable immonium $CH_2=NR_1R_2^+$ ²⁵ and $C_7H_7^+$ ions, as exemplified with the CAD spectra of $\mathbf{3}^{3+}$ and $\mathbf{3a}^{3+}$ (Table 1). Loss of benzyl radical from $\mathbf{2}^+$ and $\mathbf{3}^{3+}$ is probably accompanied or preceded by hydrogen migration within the amine moiety to give rise to the stable immonium ions, $CH_2=NH_2^+$ (m/z 30) and $CH_2=NHCH_3^+$ (m/z 44), respectively.²⁶ The corresponding nitrenium ions, CH_3NH^+ and $(CH_3)_2N^+$, due to direct benzyl loss have been calculated to be unstable in their singlet states.²⁷ The loss of a benzylic hydrogen atom, which is prominent in the electron-ionization dissociations

of $\mathbf{1}^{3+}$ – $\mathbf{3}^{3+}$ also occurs abundantly on CAD.²⁸ In addition to simple-cleavage dissociations, CAD of $\mathbf{2}^{3+}$ (Table 1) gave rise to $C_2H_4N^+$ fragments (m/z 42), which did not retain the NH hydrogen atom, as evidenced by the CAD spectrum of $\mathbf{2a}^{3+}$, which showed no mass shift due to the N-bound deuterium atom. The $C_2H_4N^+$ ion is likely to be formed by loss of the benzylic hydrogen atom followed by elimination of benzene from the $(M - H)^+$ ion. CAD of benzylamine cation radical $\mathbf{1}^{3+}$ showed predominant loss of hydrogen, while the benzylic C–N bond cleavage was a very minor process that gave rise to a weak $C_7H_7^+$ at m/z 91 (Table 1). Double hydrogen transfer to the aromatic ring gave rise to the $C_6H_7^+$ ion (m/z 79), which was abundant in the CAD spectra of both $\mathbf{1}^{3+}$ (Table 1) and of the $(M - H)^+$ ion formed from $\mathbf{1}^{3+}$ in the ion source. The $(\mathbf{1} - H)^+$ ion is a plausible intermediate in the dissociation of $\mathbf{1}^{3+}$, as the reaction $(\mathbf{1} - H)^+ \rightarrow C_6H_7^+ + HCN$ forms a stable neutral molecule. The major fragments observed in the CAD spectra were further used as signatures for ion dissociations in the $^+NR^+$ mass spectra of the cation radicals occurring following collisional reionization.

Collisional neutralization of $\mathbf{3}^{3+}$ was studied for CH_3SSCH_3 , $(CH_3)_3N$, and Xe, as exemplified with the $^+NR^+$ spectrum in Figure 1. The spectrum showed a weak peak of reionized (survivor) $\mathbf{3}^{3+}$ and abundant fragment ions at m/z 58 and 91, which were analogous to those formed by CAD (Table 1). Neutralization with $(CH_3)_3N$ gave a $^+NR^+$ spectrum which was very similar to that in Figure 1, and which agreed closely to the $^+NR^+$ spectrum of $\mathbf{3}^{3+}$ previously published by Beranova and Wesdemiotis.¹¹ The $CH_2=N(CH_3)_2^+$ and $C_7H_7^+$ ions showed clean mass shifts upon deuteration ($\mathbf{3a}^{3+}$), e.g., m/z 58 \rightarrow m/z 60 and m/z 91 \rightarrow m/z 93, which revealed negligible migration of the benzylic hydrogen atoms in dissociating $\mathbf{3}^{3+}$ and $\mathbf{3}$. The $^+NR^+$ and CAD spectra of $\mathbf{3}^{3+}$ differ most in the relative abundance of $C_2H_6N^+$ (m/z 44), whose peak is negligible in Figure 1. The immonium ion at m/z 58 and the $(M - H)^+$ ion at m/z 134 represent specific signatures for the formation of $\mathbf{3}$ under $^+NR^+$ conditions.

Neutralization–reionization of the N-methylbenzylamine cation radical $\mathbf{2}^{3+}$ gave a negligible survivor ion at m/z 121 (Figure 2a). Benzylic cleavages gave rise to $(M - H)^+$ and $C_7H_7^+$ ions, which were analogous to those in the CAD spectrum (Table 1). The $C_2H_4N^+$ ion is also prominent in the $^+NR^+$ spectrum and represents a signature fragment. In addition, $C_6H_6^+$ is an important fragment ion in $^+NR^+$, but less so in CAD. The $^+NR^+$ spectrum of the N–D derivative $\mathbf{2a}^{3+}$ (Figure 2b) shows a clean mass shift m/z 78 \rightarrow m/z 79, which indicates transfer of the amine hydrogen atom onto the aromatic ring in the formation of C_6H_6 . The fragments at m/z 120 and 78 were selected as signatures for the formation of $\mathbf{2}$ from hypervalent radicals under $^+NR^+$ conditions.

The $^+NR^+$ spectrum of $\mathbf{1}^{3+}$ shows a negligible survivor ion (Figure 2c). Benzylic cleavage of one of the C–H bonds gives rise to the $(M - H)^+$ fragment at m/z 106, whereas C–N bond cleavage to give C_7H_7 is very inefficient. The spectrum is dominated by peaks of aromatic ring fragments, which are common for the $^+NR^+$ dis-

(22) Patey, A. L.; Waldran, N. M. *Tetrahedron Lett.* **1970**, 3375.

(23) Gaussian 92, Revision C. Frisch, M. J.; Trucks, G. W.; Head-Gordon, M.; Gill, P. M. W.; Wong, M. W.; Foresman, J. B.; Johnson, B. G.; Schlegel, H. B.; Robb, M. A.; Replogle, E. S.; Gomperts, R.; Andres, J. L.; Raghavachari, K.; Binkley, J. S.; Gonzalez, C.; Martin, R. L.; Fox, D. J.; DeFrees, D. J.; Baker, J.; Stewart, J. J. P.; Pople, J. A. Gaussian, Inc., Pittsburgh, PA, 1992.

(24) McLafferty, F. W.; Stauffer, D. B. *The Wiley/NBS Registry of Mass Spectral Data*, Vol. 1; Wiley: New York, 1989; p 66, 124, 204.

(25) Bowen, R. D. *Mass Spectrom. Rev.* **1991**, 10, 225.

(26) Levens, K.; McLafferty, F. W. *J. Am. Chem. Soc.* **1974**, 96, 139.

(27) (a) Ford, G. P.; Herman, P. S. *J. Am. Chem. Soc.* **1989**, 111, 3987. (b) Falvey, D. E.; Cramer, C. J. *Tetrahedron Lett.* **1992**, 33, 1705.

(28) The $(M - H)^+$ and $(M - D)^+$ ion intensities may be affected by artifacts in the B/E-linked scans used to obtain the CAD spectra, see: (a) Morgan, R. P.; Porter, C. J.; Beynon, J. H. *Org. Mass Spectrom.* **1977**, 12, 735. (b) Busch, K. L.; Glish, G. L.; McLuckey, S. A. *Mass Spectrometry/Mass Spectrometry: Techniques and Applications of Tandem Mass Spectrometry*; VCH Publishers: New York, 1988; p 25.

Table 1. Collisionally Activated Dissociation Spectra of 1⁺, 2⁺, 2a⁺, 3⁺, 3a⁺, 4⁺, 4a⁺, and 6⁺

<i>m/z</i>	relative intensity ^a							
	1 ⁺	2 ⁺	2a ⁺	3 ⁺	3a ⁺	4 ⁺	4a ⁺	6 ⁺
135				(>100)	(>100)			(17)
134				(>100)	6.3			3
133				21	7.5			1.5
132				25	1.3			
131				3.8				
121			(>100)		1.3			
120		(>100)	(>100)	1.9	3.8			6.8
119		(56)	30	10	5			
118		(42)	12	28	6.3			1.7
117		6.5	2	6.7				
116				1.9				
110							(22)	
109							6.5	
108							4	
107			1			(18)		
106	(>100)	1.5	2.5	0.9	0.6	19		
105	10	3.5	14	3.1	0.6			
104	21	17	5.1	1.9	0.6			
103		3	1	3	0.4			
94			1	1.9	16			
93		2	3	3	66			
92		16	22	17	13	15	7	12
91	2.2	39	39	100	9.6	100	100	100
90	1.2	6	7	6.5	3	17	10	11
89	3	12	11	10		16	9	8
80	10	1.4	2			0.6	0.4	
79	100	3	4	1.3	1.3	3.6	0.8	
78	10	8	10	3.3	1.3	3.6	1	1.3
77	20	18	14	8	3	8.4	2	4
76	2	2.7	2.3	1.6		1.4	0.6	
67					3.1			
66		1	1.5		3.8			
65	2	7.3	7	9.2	1.6	7.3	4.3	6.8
64	1	2.1	2.3	1.9	1.3	2.8	1.7	1.2
63	2.6	5	5	4.4	1.3	7	3.8	3
62	1.3	1.6	1.8	1.4		2.5	1.4	
60		1	1		100			
59		1	1	1.3	6.5			
58				81	1.5			19
57				3.4				
56							2.4	
55							1.6	
53		1	1.5					
52	3.6	3.5	3.4	1.3	1.3	2.5	1.2	1.2
51	6.6	10	10	5	2.5	7.3	3.8	4.3
50	3.4	5	5	3.1	1.3	4.7	2.6	2.1
49								
45			11		2.1			5.5
44		14	9	52	65			27
43		4.5	6.4	2.5	9			1.7
42		100	100	20	5			6.5
41		2	2					
39	2	4	4	3	1.3	4.6	3	2.9
38							1.1	
32							1.3	
31			40					
30		47	27			2.4		
29			2				1.0	
28	7.4	3	1.5					

^a Integrated peak areas relative to that of the most abundant peak, excluding (M - nH)⁺.

sociations of 1–3. The (M - H)⁺ ion at *m/z* 106 is the only unique signature for 1.

The ⁺NR⁺ mass spectra of cation radicals 7⁺ (Figure 3a) and 8⁺ (Figure 4a) show deep dissociations of the aromatic rings that occur upon collisional electron transfer. Ion dissociations of 7⁺ in CAD are straightforward and comprise loss of H[•] (*m/z* 224), benzylic C–N bond cleavage (*m/z* 181), and loss of the pentafluorophenyl group (*m/z* 58, Table 2). These ion dissociations are analogous to those observed for the unsubstituted ion 3⁺. By contrast, neutralization–reionization of 7⁺ results in a pronounced fission of the pentafluorobenzene ring to

yield a series of fluorinated carbon clusters, e.g., C₅F₃⁺ (*m/z* 117), C₅F₂⁺ (*m/z* 98), C₃F₃⁺ (*m/z* 93), C₄F₂⁺ (*m/z* 86), C₅F⁺ (*m/z* 79), C₃F₂⁺ (*m/z* 74), C₂F₂⁺ (*m/z* 62), and CF⁺ (*m/z* 31), with the peak of the latter fragment dominating the spectrum (Figure 3a). The cleavage of the C₆F₅–CH₂ bond, which is abundant in ion dissociations, is negligible on ⁺NR⁺ as evidenced by the very small peak of CH₂=N(CH₃)₂⁺ at *m/z* 58 and the absence of the complementary C₆F₅⁺ (*m/z* 167) fragment (Figure 3a). Cleavage of the benzylic C–N bond gives rise to C₆F₅CH₂⁺ (*m/z* 181) and C₂H₄N⁺ (*m/z* 42). It should be noted that C₆F₅CH₂[•] is a stable radical under ⁺NR⁺

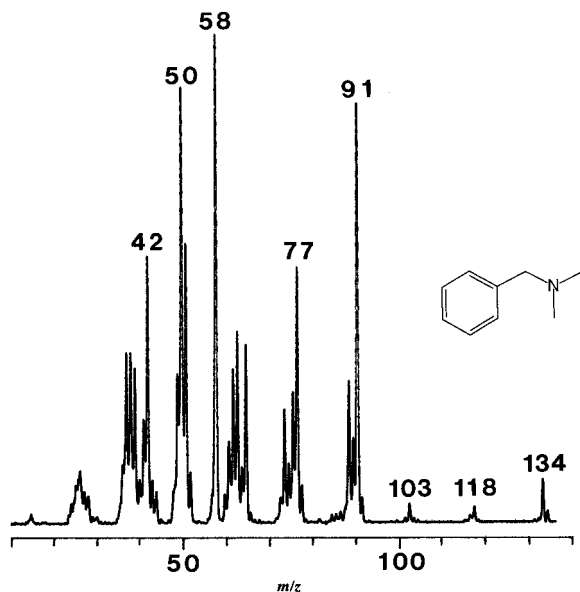


Figure 1. Neutralization–reionization ($\text{CH}_3\text{SSCH}_3/\text{O}_2$) spectrum of 3^+ .

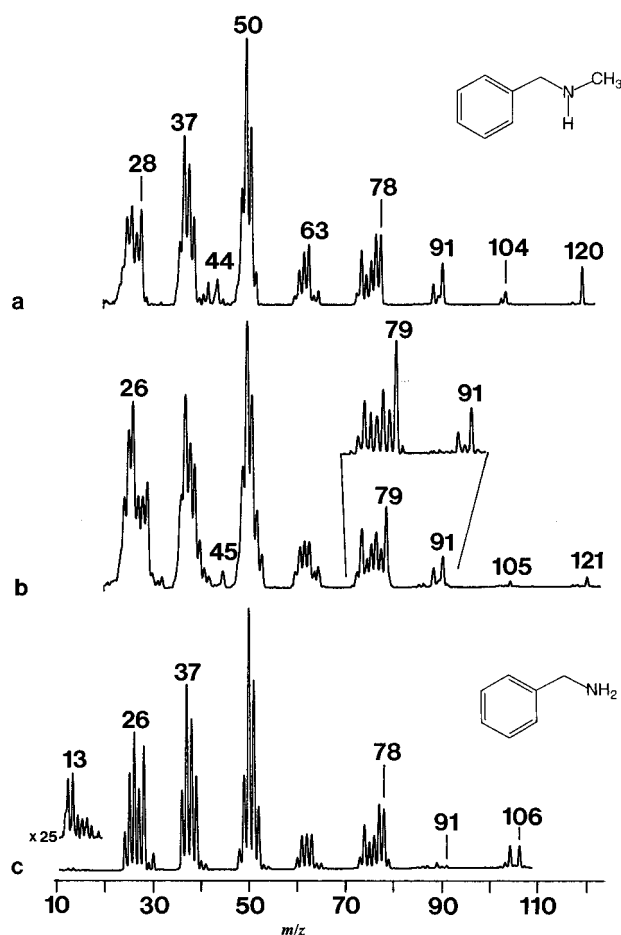


Figure 2. Neutralization–reionization ($\text{CH}_3\text{SSCH}_3/\text{O}_2$) spectra of top (a) 2^+ , middle (b) $2a^+$, and bottom (c) 1^+ .

conditions as the $^+\text{NR}^+$ spectra of the $\text{C}_7\text{H}_2\text{F}_5^+$ cations generated from **7** and $\text{C}_6\text{F}_5\text{CH}_2\text{F}$ showed significant survivor ions (Figure 3b). Furthermore, dissociations of $\text{C}_7\text{H}_2\text{F}_5^+$ on $^+\text{NR}^+$ give fragments that are very similar to those found in the $^+\text{NR}^+$ spectrum of amine **7**. This indicates that the cleavage of the benzylic C–N bond in **7** could be an important process in spite of the low

intensity of the reionized $\text{C}_7\text{H}_2\text{F}_5^+$ intermediate. The sensitivity of $\text{C}_7\text{H}_2\text{F}_5^+$ to collisional activation was tested by recording the $^+\text{NR}^+$ spectra at 70% and 90% transmittances in the neutralization and reionization steps, which corresponded to 95% and 85% single-collision conditions, respectively. The spectra showed practically no change between 90%/90% and 70%/90% $^+\text{NR}^+$ conditions, which gave 3.75% and 3.80% of surviving $\text{C}_7\text{H}_2\text{F}_5^+$ relative to the total NR intensities (ΣI_{NR}). At the 70%/70% transmittance the relative intensity of $\text{C}_7\text{H}_2\text{F}_5^+$ decreased to 3.25% ΣI_{NR} . This indicates that $\text{C}_7\text{H}_2\text{F}_5^+$ ions are somewhat more sensitive to collisional activation with O_2 than are $\text{C}_7\text{H}_2\text{F}_5^+$ radicals to collisional activation with CH_3SSCH_3 , although the overall effect is rather weak.

The CAD and $^+\text{NR}^+$ spectra of $\text{C}_7\text{H}_2\text{F}_5^+$ ions are very different. The former shows mostly sequential elimination of HF molecules (m/z 161 and 131) and acetylene (m/z 155), whereas neutralization results in more pronounced ring dissociations combined with losses of fluorine atoms. Note that elimination on CAD of CF^+ radical is a very minor process in the ion dissociations of 7^+ and $\text{C}_7\text{H}_2\text{F}_5^+$ (Table 2). The predominating CF^+ fragment in the $^+\text{NR}^+$ spectra thus cannot be accounted for by reionization of neutral CF^+ formed by concurrent CAD of 7^+ ion in the neutralization collision cell. By contrast, reionization of CF^+ from neutral dissociations may contribute to the efficient detection of CF^+ as the ionization cross section of the CF^+ radical is greater than those of some more highly fluorinated species.²⁹

It is worth noting that the differences in the CAD and $^+\text{NR}^+$ spectra of the $\text{C}_7\text{H}_2\text{F}_5^+$ ions may possibly come from sampling different mixtures of isomeric structures for ion and neutral dissociations as is known for the benzyl and tropylium isomers in the C_7H_7^+ and $\text{C}_7\text{H}_6\text{F}^+$ systems.^{30,31} Ab initio calculations (Table 3) indicate that the 1,2,3,4,5-pentafluorotropylium ion is ca. 24 kJ mol^{-1} more stable than the 2,3,4,5,6-pentafluorobenzyl ion at 298 K. A benzyl–tropylium isomerization of the ions is therefore possible, although the energy difference in the pentafluoro system is much smaller than that in unsubstituted C_7H_7^+ (48 kJ mol^{-1}).³⁰ Isomerization in the pentafluorobenzyl cation may face a larger energy barrier than that in the benzyl cation, as discussed for the monofluorobenzyl and tropylium ions.³¹ By contrast, the pentafluorotrotyl radical is calculated to be 87 kJ mol^{-1} less stable than its pentafluorobenzyl isomer at 298 K (Table 3), and so the latter should not isomerize when formed by dissociations of neutral intermediates. Both the pentafluorobenzyl and pentafluorotrotyl radicals show only small energy differences between the corresponding optimized neutral structures and those formed by vertical electron attachment (3.5 and 29 kJ mol^{-1} , respectively, Table 3), indicating small vibrational excitation through Franck–Condon effects.

A still different picture emerges from the CAD and $^+\text{NR}^+$ dissociations of cation radical **8**⁺ (Figure 4a). Ion dissociations are dominated by the aryl– CH_2 bond cleav-

(29) (a) Tarnovsky, V.; Becker, K. *J. Chem. Phys.* **1993**, *98*, 7868. (b) The analogous CCl^+ shows a moderate $^+\text{NR}^+$ efficiency, 0.0018: Gu, M.; Turecek, F. *Org. Mass Spectrom.* **1993**, *28*, 1135.

(30) From $\Delta H_f(\text{benzyl}^+) = 919 \text{ kJ mol}^{-1}$, $\Delta H_f(\text{tropylium}^+) = 871 \text{ kJ mol}^{-1}$, see: (a) Baer, T.; Morrow, J. C.; Shao, J. D.; Olesik, S. *J. Am. Chem. Soc.* **1988**, *110*, 5633. (b) Lifshitz, C.; Gotkis, Y.; Ioffe, A.; Laskin, J.; Shaik, S. *Int. J. Mass Spectrom. Ion Processes* **1993**, *125*, R7. For a recent review of C_7H_7^+ isomers, see: (c) Lifshitz, C. *Acc. Chem. Res.* **1994**, *27*, 138.

(31) McLafferty, F. W.; Amster, I. J. *J. Fluorine Chem.* **1981**, *18*, 375.

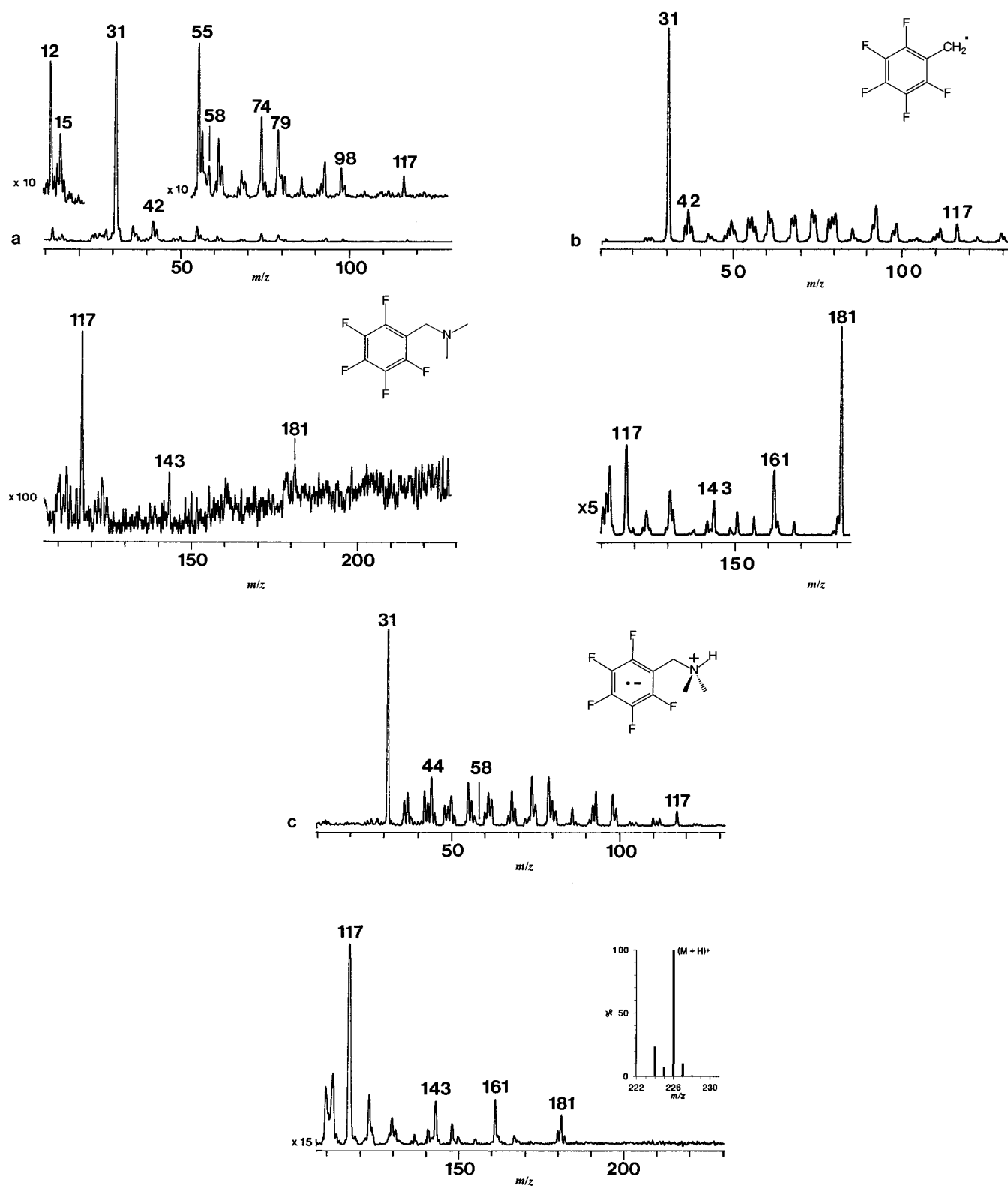


Figure 3. Neutralization–reionization (CH_3SSCH_3/O_2) spectra of (a) 7^+ , (b) $C_7F_5H_2^+$, and (c) 9^+ .

age, giving the $CH_2=N(CH_3)_2^+$ ion at m/z 58 (Table 2). Benzylic C–N bond cleavage with loss of neutral $\cdot N(CH_3)_2$ gives the ion at m/z 181, which further eliminates NO_2 (m/z 135 and 89). A competing elimination of HNO_2 and NO_2 from 8^+ gives rise to ions at m/z 178 and 132, respectively. CAD of the intermediate 3,5-dinitrobenzyl ion (or its tropylium isomers, m/z 181) is consistent with this interpretation, showing sequential losses of NO_2 to form fragments at m/z 135 and 89 (Table 2).

In contrast to CAD, $^+NR^+$ of 8^+ results in the dominant formation of NO , which gives rise to the peak of NO^+ at m/z 30 (Figure 4a). Note that neutral NO is not eliminated by CAD of 8^+ (Table 2) nor from its nitro-group-containing fragments. Hence the formation of NO on $^+NR^+$ cannot be accounted for by reionization of neutral fragments from ion dissociations concurrent with neutralization. By comparison, NO_2 which is eliminated by ion CAD (Table 2) gives rise to a much smaller peak

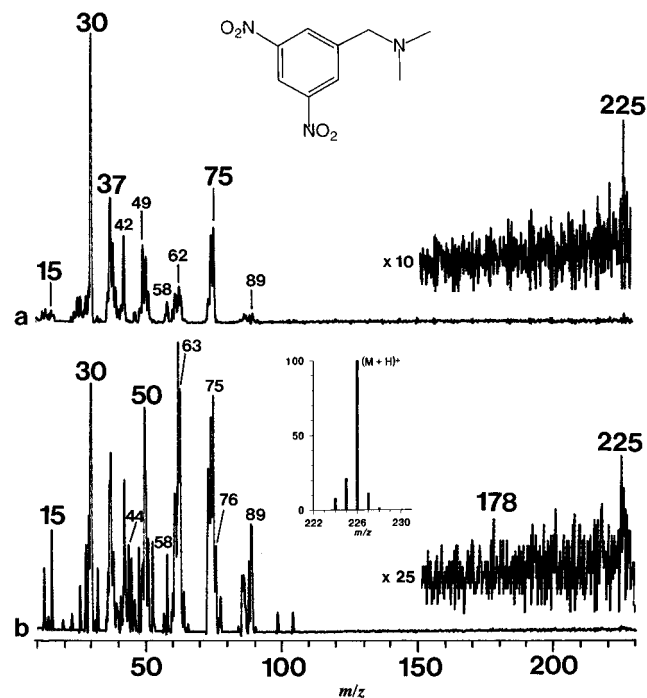


Figure 4. Neutralization–reionization ($\text{CH}_3\text{SSCH}_3/\text{O}_2$) spectra of top (a) 8^+ and bottom (b) 10^+ .

at m/z 46 after reionization. In contrast to the case of 3^+ and 7^+ , $^+\text{NR}^+$ of 8^+ shows a very small but detectable survivor ion, suggesting stabilization in the intermediate neutral 8 or reionized 8^+ .

Hypervalent Radicals. Neutralization of ammonium ions by collisions with CH_3SSCH_3 , $(\text{CH}_3)_3\text{N}$, and Xe was studied for 6^+ prepared by gas-phase protonation of 3 with NH_4^+ and C_4H_9^+ . Both these gas-phase acids protonate 3 selectively at the nitrogen atom, as the gas-phase basicity of the aromatic system is too low to permit ring protonation with NH_4^+ or C_4H_9^+ .³² However, protonation with C_4H_9^+ ($\Delta\text{PA} = 152 \text{ kJ mol}^{-1}$) is more exothermic than that with NH_4^+ ($\Delta\text{PA} = 103 \text{ kJ mol}^{-1}$),³³ resulting in somewhat higher vibrational excitation in the 6^+ formed.

The dissociations of hypervalent 6^+ proceed by benzylic $\text{CH}_2\text{--N}$ bond homolysis, as evidenced by the reionized C_7H_7^+ and $(\text{CH}_3)_2\text{NH}^+$, and by cleavage of the N--H bond, as evidenced by the presence of the signature ions at m/z 58 from reionization of the intermediate 3 (Figure 5a). The branching ratios for the N--H and $\text{CH}_2\text{--N}$ bond cleavages in hypervalent 6^+ depend on the precursor ion internal energy. Neutralization of the more energetic ions from protonation by C_4H_9^+ led to less hydrogen loss as judged by the small peak of the signature ion at m/z 58. Exact quantification of the branching ratios is hampered by the unknown reionization efficiencies and their dependence on neutral internal and kinetic energy.³⁴ However, it appears from the relative abundances of the signature ions that the benzylic $\text{CH}_2\text{--N}$ bond cleavage is the prevalent dissociation of hypervalent 6^+ . Surprisingly, dissociations by N--CH_3 bond cleavage are much less significant in 6^+ , as evidenced by the very low

(32) Lias, S. G.; Bartmess, J. E.; Liebman, J. F.; Holmes, J. L.; Levin, R. D.; Mallard, G. W. *J. Phys. Chem. Ref. Data* **1988**, *17*, Supplement 1.

(33) From $\text{PA}(3) = 954 \text{ kJ mol}^{-1}$, $\text{PA}(\text{NH}_3) = 851.4 \text{ kJ mol}^{-1}$, and $\text{PA}(i\text{-C}_4\text{H}_9) = 802 \text{ kJ mol}^{-1}$; see: Szulejko, J. E.; McMahon, T. B. *J. Am. Chem. Soc.* **1993**, *115*, 7839.

(34) Harnish, D.; Holmes, J. L. *Org. Mass Spectrom.* **1994**, *29*, 213.

Table 2. Collisionally Activated Dissociation Spectra of 7^+ , 8^+ , 9^+ , 10^+ , $\text{C}_7\text{H}_2\text{F}_5^+$, and $\text{C}_7\text{H}_5\text{N}_2\text{O}_4^+$

m/z	relative intensity			m/z	relative intensity		
	7^+	9^+	$\text{C}_7\text{H}_2\text{F}_5^+$		8^+	10^+	$\text{C}_7\text{H}_5\text{N}_2\text{O}_4^+$
225		(>100)		225	(10)		
224	(>100)	25		224	(75)	5	
223		4.6		211		4	
211		1.3		210		15	
210		8.5		209		13	
209		3.7		208	7	10	
208	5.1	1.6		194		3	
207		5.2		184		11	
204	3.5	1.1		183		70	
193	1.3			182	5	10	
192	5.9			181	31	51	
190	1.5	1.6		180	1	39	(>100)
182	11	9.4		179	6	6.6	(>100)
181	100	100		178	28	17	14
180	1.2	9	(30)	166	1	13	
179			3	165	1	6	3
167	1.5	2.7	2.7	164		7.5	
164	1.4			136	1	7.5	7.2
163	5.1	4.5	4	135	7	28	100
162	1.7	4.5	12	134		35	11
161	3.8	6.5	100	133	2	6	20
155	1.1	1.9	12	132	16	20	57
150			7.5	131	2	4	5
143	1.5	3.1	6	120	1	5.4	1.4
137		1	4	119		6.6	
132			5	118	2	11	
131	1.1	2	28	117	1	3.5	2.8
130	1.1	1.6	11	105		3.7	1.6
117	2.4	4.1	10	104		5	1.4
112	1.1	2.2	9	91	1	6	2
111			5	90	1.7	14	5
99	1.2	2	7.5	89	8	43	36
98		1	2.5	88	1.5	7	9
93	2	4	16	78		6	1
81	1	2	9	77	2.2	11	8
80			4	76	1	6	4.3
75	1.2	1.8	8.7	75	2.3	13	5
74			4.4	65		5	3
69	1.1	2.3	12	63		18	13
58	50	17		62	1.2	7	6
57	2.7	1.8	3.2	59	5	6.5	
51		1	5.5	58	100	100	
45		4.8		51		5.5	2
44		18		50		4	1.7
43	1.9	2.4		45		17	
42	7.5	5.4		44	1	77	
31	0.9	1.6	16	43		6	
				42	3.5	13	3
				30	1	5	

Table 3. Total Energies of 2,3,4,5,6-Pentafluorobenzyl and 1,2,3,4,5-Pentafluorotropyli Cations and Radicals

species	energy ^a		ZPVE ^b	H_{298}^- $\text{H}_0^{b,c}$	IE_a^d	RE_v^e
	3-21G	6-31G(d)				
$\text{C}_6\text{F}_5\text{CH}_2^+$	-758.90926	-763.06379	199	28		7.84
$\text{C}_6\text{H}_6\text{CH}_2^+$	-759.21722	-763.35311	188	29		7.98
$\text{C}_6\text{F}_5\text{CH}_2^*$		-763.35179				
(VN) ^f						
$\text{F}_5\text{-tropyli}^+$	-758.91142	-763.07343	201	27		6.40
$\text{F}_5\text{-tropyli}^*$	-759.17506	-763.31967	187	29		6.82
$\text{F}_5\text{-tropyli}^*$		-763.30857				
(VN) ^f						

^a Hartree: 1 hartree = 2625.5 kJ mol⁻¹. ^b From 3-21G harmonic frequencies scaled by 0.9, units of kJ mol⁻¹. ^c 298 K enthalpy corrections calculated with the rigid-rotor-harmonic oscillator approximation. ^d Adiabatic ionization energies from HF/6-31G(d) calculations and ZPVE corrections, units of eV. ^e Vertical recombination energies from HF/6-31G(d) calculations, units of eV. ^f Single-point calculations on optimized ion geometries.

relative abundances of the signature ions at m/z 120 and 78 from reionization of the intermediate 2 (Figure 5a). Note that the total yields for neutralization and reion-

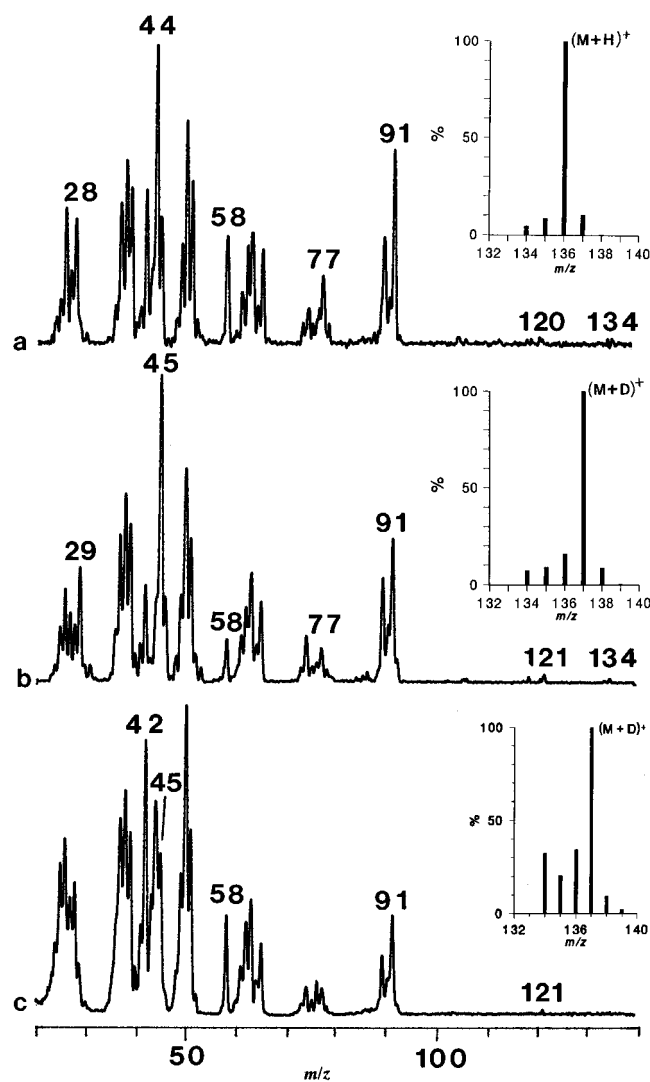


Figure 5. Neutralization–reionization (CH_3SSCH_3/O_2) spectra of top (a) NH_4^+ -protonated $6b^+$, middle (b) ND_4^+ -deuterated $6b^+$, and bottom (c) $C_4D_9^+$ -deuterated $6b^+$.

ization of 2^+ are greater than those for 3^+ ,³⁵ indicating that the reionization efficiency of 2 should not be significantly smaller than that of 3 . Hence the low yield of reionized 2^+ is not due to a discrimination upon reionization, but rather can be attributed to the inefficient formation of neutral 2 in dissociations of the hypervalent radical 6^* . By comparison, N– CH_3 bond cleavages do occur in hypervalent aliphatic ammonium radicals $CH_3NH_3^*$,² $(CH_3)_2NH_2^*$,⁹ and $(CH_3)_3NH^*$.¹⁰

N-Deuteration with ND_4^+ or $C_4D_9^+$ appears to have opposite effects on the branching ratios for the N–D and CH_2 –N bond cleavages in $6b^*$ (Figure 5b). N–D bond cleavage in ND_4^+ -deuterated $6b^*$ is relatively suppressed, whereas the same cleavage in the $C_4D_9^+$ -deuterated $6b^*$ is relatively enhanced (Figure 5c). These effects show that the branching ratios for N–H and CH_2 –N bond dissociations depend on the precursor ion internal energy; however, the mechanism of these energy effects is not clear. Loss of CH_3 remains a minor dissociation pathway in $6b^*$ as judged from the weak signature ions at m/z 121 and 79. However, no overall stabilization through

(35) The $CH_3SSCH_3(70\%T)/O_2(70\%T)^+NR^+$ efficiencies, expressed as the sum of $^+NR^+$ ion intensities relative to that of the unattenuated incident precursor ion beam) were as follows: 2^+ , 0.0028; 3^+ , 0.00046; $(CH_3)_2NH$, 0.0012.

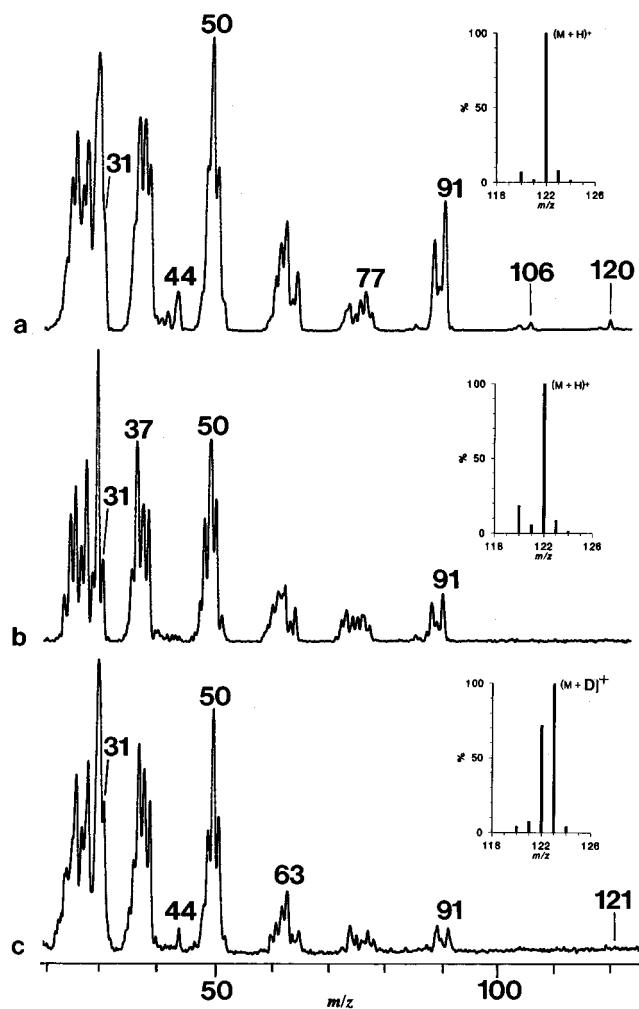


Figure 6. Neutralization–reionization (CH_3SSCH_3/O_2) spectra of top (a) NH_4^+ -protonated 5^+ , middle (b) $C_4H_9^+$ -protonated 5^+ , and bottom (c) $C_4D_9^+$ -deuterated $5a^+$.

isotope effects of hypervalent $6b^*$ is observed that would lead to the detection of a survivor ion at m/z 136. Deuterium labeling in the benzylic group has no major affect on the dissociations of $6a^*$. The label remains localized in the benzylic group as shown by the clean mass shifts of m/z 91 \rightarrow m/z 93 and m/z 58 \rightarrow m/z 60.

Neutralization with CH_3SSCH_3 of ammonium ion 5^+ provides $^+NR^+$ spectra (Figure 6a,b) that slightly depend on the precursor ion internal energy. Neutralization of 5^+ prepared by the more exothermic protonation with $C_4H_9^+$ (Figure 6b) results in more extensive CH_2 –N benzylic cleavage compared to that in 5^+ prepared by protonation with NH_4^+ (Figure 6a). This is documented by the relative abundances of the signature ions for H loss (m/z 44) and benzylic cleavage (m/z 91) in the corresponding spectra (Figures 6a,b). The $^+NR^+$ spectrum of NH_4^+ -protonated 5^+ shows fragments at m/z 120, 104, and 44, typical for the $C_6H_5CH_2NHCH_3$ intermediate, signifying loss of the ammonium hydrogen from the hypervalent radical 5^* (Figure 6a). Loss of methyl is indicated by the presence of the $C_6H_5CH=NH_2^+$ fragment at m/z 106, which is a signature for the intermediate 1 . This shows that all the bonds adjacent to the hypervalent nitrogen center in 5^* dissociate to some extent, contrasting thus the behavior of 6^* (vide supra). Deuterium labeling in $5a^+$ results in a negligible shift of m/z 44 to 45 and the absence of deuterium incorporation in most fragments except for CH_3NH_2 (Figure 6c). This shows

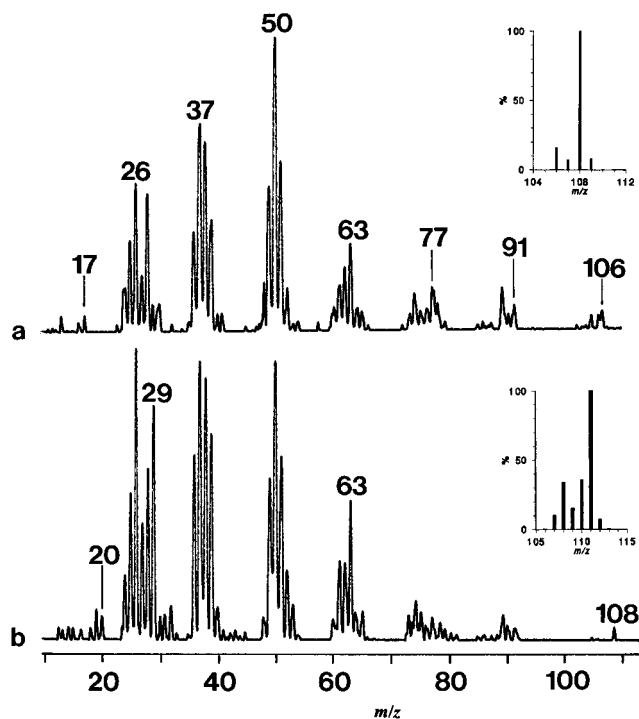


Figure 7. Neutralization–reionization ($\text{CH}_3\text{SSCH}_3/\text{O}_2$) spectra of top (a) 4^+ and bottom (b) $4a^+$.

that D and not H is lost preferentially from hypervalent $5a^+$, indicating an inverse deuterium isotope effect. Inverse isotope effects on dissociations of hypervalent radicals have been noted previously.^{12,36} In the absence of detailed potential energy surfaces for the dissociations of 5^+ and 6^+ , the origin of these inverse isotope effects remains unclear.

Neutralization of the simplest benzylammonium ions 4^+ and $4a^+$ induces mostly N–H bond cleavage, whereas the formation of C_7H_7 and NH_3 by CH_2 –N bond cleavage is much less abundant. The N–H bond dissociation is indicated by the benzylamine signature ions at m/z 106, 78, and 30 (Figure 7a) and their deuterio analogs at m/z 108, 79–81, and 32 (Figure 7b). The CH_2 –N benzylic cleavage is indicated by the complementary C_7H_7 and NH_3 fragments. While the formations from $4a$ of C_7H_7^+ by neutral or ion dissociations are not accompanied by H/D exchange, as corroborated by the unshifted m/z 91 in both the $^+\text{NR}^+$ and CAD spectra, the ND_3 peak at m/z 20 shows an accompanying peak at NHD_2 at m/z 19. The origin of the latter fragment is unclear, as H/D exchange between $\text{C}_6\text{H}_5\text{CH}_2$ and ND_3 is excluded by the clean formation of the complementary C_7H_7^+ . We tentatively explain the formation of NHD_2 as being due to an artifact from the fragmentation of the d_2 isotopomer of $4a^+$ ($\text{C}_6\text{H}_5\text{CH}_2\text{NHD}_2^+$, m/z 110, Figure 7b, inset), which is cofragmented and cotransmitted with $4a^+$.

The unusually small peak of C_7H_7^+ from 4^+ raised the question of the stability of the intermediate benzyl radical under $^+\text{NR}^+$ conditions.³⁷ We carried out a series of measurements in which C_7H_7^+ ions from benzyl bromide were neutralized with CH_3SSCH_3 and reionized with O_2 under single and multiple collision conditions. All these spectra showed substantial peaks of reionized C_7H_7^+ (16%

ΣI_{NR}), attesting to the stability of the vertically neutralized benzyl radical (these spectra are given as supporting information). The effects of collisional reionization were also studied. Benzyl radical was prepared as a neutral fragment by collision-induced dissociation with He of stable 1,2-diphenylethane cation radical and subsequently reionized to C_7H_7^+ by collisions with oxygen. The resulting spectrum again showed a strong peak of surviving C_7H_7^+ (19% ΣI_{NR} , supporting information). This indicates that the small peak of C_7H_7^+ in the $^+\text{NR}^+$ spectrum of 4^+ originates from inefficient loss of ammonia to form the benzyl radical and not from an instability of the latter.

Neutralization of the fluorinated ammonium ion 9^+ results in the dissociation of the benzylic bond as indicated by the reionized $\text{C}_2\text{H}_6\text{N}^+$, $\text{C}_2\text{H}_7\text{N}^+$, and $\text{C}_6\text{F}_5\text{CH}_2^+$ fragments at m/z 44, 45, and 181, respectively (Figure 3c). Loss of the ammonium hydrogen atom is negligible, as shown by the very small peaks of reionized $\text{CH}_2=\text{N}(\text{CH}_3)_2^+$ and C_6F_5^+ at m/z 58 and 167, respectively. Loss of methyl is difficult to distinguish due to an overlap of the presumed $\text{CH}_2=\text{NHCH}_3^+$ signature ion with the isobaric fragment from reionized dimethylamine. Nevertheless, the very small relative abundance of CH_3^+ suggests that loss of methyl from 9^+ is not important.

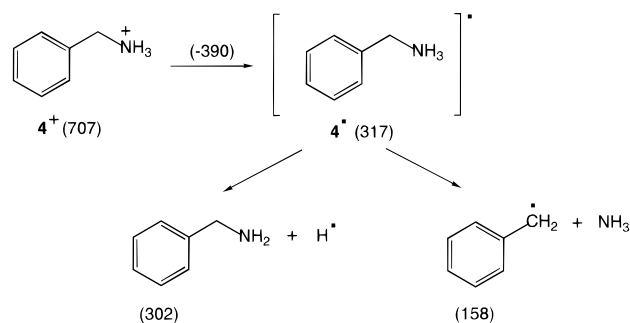
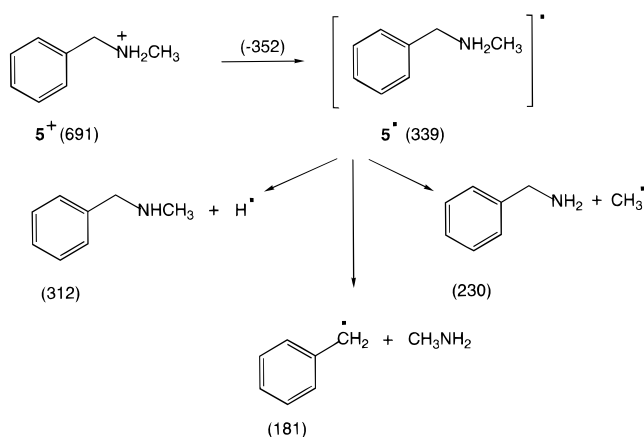
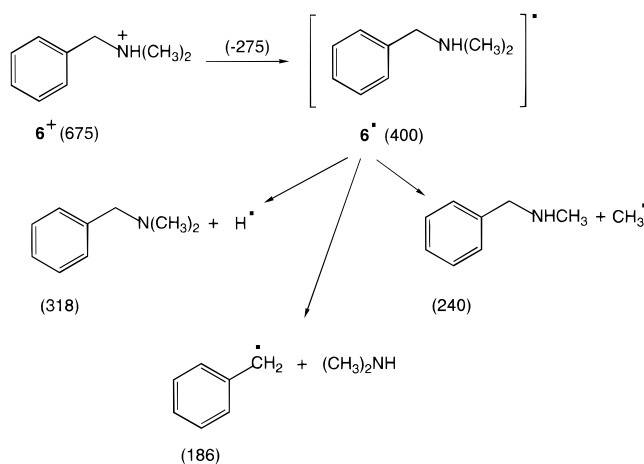
Neutralization of ion 10^+ results in a spectrum (Figure 4b) which is qualitatively different from those of the other ammonium ions. Radical 10^+ shows little dissociation of the benzylic CH_2 –N bond, as indicated by the modest relative abundances of the dimethylamine ions at m/z 45 and 44. The loss of H from 10^+ is indicated by the weak peak of reionized 8^+ (m/z 225) and the $\text{CH}_2=\text{N}(\text{CH}_3)_2^+$ fragment at m/z 58. When compared with the $^+\text{NR}^+$ dissociations of cation radical 8^+ , those of 10^+ show mass shifts of the aromatic fragments, e.g., m/z 37 to m/z 38, m/z 49 to m/z 50, m/z 62 to m/z 63, and (in part) m/z 75 to m/z 76 (Figure 4b). These are indicative of dissociations involving hydrogen transfer from the ammonium group to the aromatic ring that takes place either in the intermediate neutral or following reionization. Note, however, that the ring-cleavage dissociations are much less abundant in CAD of 10^+ (Table 2), so their occurrence on $^+\text{NR}^+$ is likely to be due to fragmentations of the neutral intermediate 10^+ .

Discussion

The dissociations of hypervalent radicals 4^+ – 6^+ , 9^+ , and 10^+ show effects of methyl substituents at the amine nitrogen atom and fluorine and nitro substituents in the aromatic ring. Substitution by methyls at the amino group relatively enhances cleavage of the CH_2 –N bond, which occurs predominantly in 6^+ but less so in 5^+ and 4^+ . It is noteworthy in this respect that CH_2 –N bond heterolysis upon CAD of ammonium cations is much less sensitive to methyl substitution at the leaving amine moiety as shown for 4^+ and 6^+ (Table 1). Cleavage of the N– CH_3 bond increases from 6^+ to 5^+ , in spite of the less favorable statistical factor in the latter, and competes with the N–H bond cleavage. The latter dominates in the dissociations of 4^+ , where it outcompetes the CH_2 –N bond cleavage. It should be noted that the product relative abundances provide relative propensities to bond cleavage but do not allow direct determination of bond dissociation energies. In relative terms, methyl substituents at the amino group do affect bond dissociations but do not increase the lifetimes of the hypervalent am-

(36) Wesdemiotis, C.; Fura, A.; McLafferty, F. W. *J. Am. Soc. Mass Spectrom.* **1991**, *2*, 459.

(37) Buschek, J. M.; Holmes, J. L. *Org. Mass Spectrom.* **1988**, *23*, 765.

Scheme 3**Scheme 4****Scheme 5**

monium intermediates to make them metastable on the microsecond time scale.

The energetics of bond dissociations in **4**⁺–**6**⁺ can be roughly estimated from the known heats of formation of the cations and neutral products and the estimated ionization energies of analogous primary, secondary, and tertiary ammonium ions, e.g., 4.0, 3.6, and 2.9 eV for **4**⁺, **5**⁺, and **6**⁺, respectively.^{3c} The energy data in kJ mol⁻¹ are given in Schemes 3–5 as heats of formation of the reactants and products.³² Scheme 3 shows that both the N–CH₂ and N–H bond homolyses are exothermic, such that **4**⁺ is metastable with respect to these dissociations. Thermochemical data also show that **5**⁺ and **6**⁺ are metastable with respect to N–H, N–CH₃, and CH₂–N bond homolyses of increasing exothermicity in the same order (Schemes 4 and 5). The observed absence of **4**⁺–**6**⁺ of microsecond lifetimes is consistent with these exothermic dissociation channels and indicates that there are only small activation energy barriers for the bond ho-

molyses. However, the *relative* propensities for bond cleavages in **4**⁺–**6**⁺ do not correlate with the dissociation exothermicities. For example, dissociation of the CH₂–N bond in **4**⁺ is substantially more exothermic than the N–H bond cleavage, yet the latter dissociation prevails in vertically neutralized **4**⁺. Likewise, loss of methyl from **6**⁺ is more exothermic than that from **5**⁺; yet this dissociation is relatively more abundant in the latter radical.

These results show that the cleavages of N–H and N–C bonds do not follow the usual pattern of competitive dissociations occurring on the same potential energy surface, for which a correlation between the activation energy and reaction thermochemistry could be expected. It appears that two or more electronic states are accessed by vertical reduction of ammonium cations and that these dissociative states may show specific propensities to N–H and N–C bond cleavages. The observed substituent effects are then likely to be determined by the populations of the electronic states of the given reactivity. This interpretation is consistent with previous studies of aliphatic hypervalent onium radicals that indicated that X–H bond homolysis (X = N, O) should dominate in the ground electronic state, whereas X–C bond cleavages become competitive in some excited states.^{8,10} The nature of the electronic states that are involved in the formation of radicals **4**⁺–**6**⁺ and lead to N–C bond dissociations is difficult to investigate by experiment or theory, and thus no specific conclusions regarding their reactivity can be drawn at this stage.

Electron-withdrawing substituents in the aromatic ring apparently hamper dissociations of the N–CH₃ and N–H bonds in **9**⁺ and even the cleavage of the CH₂–N bond in **10**⁺. Instead, the hypervalent radicals undergo deep fissions of the aromatic rings combined with losses of substituents. The electronic properties of the aromatic rings thus clearly have an effect on the dissociations of bonds adjacent to the ammonium nitrogen atom.

Aromatic ring fissions are common in the dissociations of **4**⁺–**6**⁺, **9**⁺, and **10**⁺, where they give rise to abundant hydrogenated or fluorinated C₄, C₃, and C₂ fragments. It is noteworthy that ring fissions in aromatic hydrocarbons are highly endothermic decompositions that are known to occur in high-energy processes such as in shock-tube experiments³⁸ or following multiphoton excitation.³⁹ For example, the dissociation C₆H₅CH₂⁺ → C₄H₂⁺ + C₃H₃⁺ + H₂, which yields the observed fragments at *m/z* 50 and 39, is 579 kJ mol⁻¹ endothermic.³² These endothermic ring fissions sharply contrast the substantially exothermic dissociations of bonds in the vicinity of the hypervalent nitrogen atom (Schemes 3–5). Reactions of such widely different thermochemistries clearly cannot occur competitively on the same potential energy surface. We consider two types of effects that can contribute to the ring fissions observed for neutralized hypervalent radicals.

First, ring fissions probably take place in a fraction of highly energetic primary neutral fragments, e.g., benzyl radicals, substituted benzyls, or benzylamines, or in their corresponding cations following collisional reionization. The energy needed for the ring fission can be supplied in part by the exothermicity of the benzyl radical formation (Schemes 3–5) but can also come from electronic

(38) Lifshitz, A. Private communication.

(39) (a) Grottemeyer, J.; Schlag, E. W. *Angew. Chem., Int. Ed. Engl.* **1988**, *27*, 447. (b) Boesl, U.; Neusser, H. J.; Schlag, E. W. *J. Chem. Phys.* **1980**, *72*, 4327. (c) Dietz, W.; Neusser, H. J.; Boesl, U.; Schlag, E. W. *Chem. Phys.* **1982**, *66*, 105.

excitation upon collisional electron transfer.^{7b} By comparison, endothermic neutralizations of $C_7H_7^+$ ions with nitrogen, oxygen, or xenon result in substantial ring fissions in the radicals formed or in their reionized counterparts.^{5e}

Second, electron capture in the cation may occur in one of the unoccupied orbitals at the aromatic ring and induce dissociations remote from the ammonium functionality. Such zwitterionic states resemble electron-transfer complexes¹⁵ in which the anionic and cationic groups are separated and which are destabilized by an excitation energy approximated by $\Delta E \approx RE(\text{cation}) - IE(\text{anion})$. The recombination energies (RE, taken as positive values) of the ammonium groups are close in magnitude to the ionization energies of the corresponding hypervalent ammonium radicals (2.9–4.0 eV).^{3e,10} The ionization energies (IE) of aromatic anions, which can be approximated by the corresponding electron affinities, are typically <2.0 eV. Hence the zwitterionic states produced by electron attachment must be inherently unstable toward intramolecular electron or proton transfer that would quench the zwitterion or to unimolecular dissociation. Unfortunately, the electronic states in the neutralized intermediates are not probed directly by the present experiments. However, the electron capture mechanism is qualitatively consistent with the increased ring fission in 9^\bullet and 10^\bullet . Both fluorine and nitro substituents increase the electron affinity (EA) of the benzene ring, e.g., EA = 0.52 and 1.65 eV in hexafluorobenzene and *m*-dinitrobenzene, respectively.¹⁸ For 9^\bullet , electron capture by the pentafluorophenyl ring should form a loosely bound electronic state, which can relax by exothermic electron transfer to the ammonium group to trigger its dissociations, e.g., cleavage of the benzylic CH_2-N group, as observed. However, most dissociations in 9^\bullet occur in the aromatic ring, suggesting another mechanism of excitation. We postulate that electron capture may occur in the dense manifold of Rydberg ns, np, and nd states, which are interspersed with valence shell excited states in fluorobenzenes.⁴⁰ Internal conversion in such an excited state will deposit sufficient vibrational energy to drive the highly endothermic ring cleavages in 9^\bullet . The formation of CF by ring fission in 9^\bullet finds an analogy in the laser photolysis of hexachlorobenzene⁴¹ or core-electron excitation of 1,1,1-trifluoroethane and 1,1-difluoroethane.⁴²

Dinitro derivative 10^\bullet shows abundant loss of NO and hydrogen transfer from the side chain onto the aromatic ring. We attribute these distinct properties to electron

capture by the aromatic ring in a fraction of neutralized 10^\bullet . As discussed by Radom and co-workers,⁴³ nitro groups, which are both σ - and π -acceptors, lower the energy of the benzene SOMO by π -delocalization, allowing thus a large portion of the negative charge to flow into the NO_2 group. This negative charge increases the reactivity of the nitro group; for example, *m*-dinitrobenzene anion radicals⁴⁴ show a dominant loss of NO that parallels that observed for 10^\bullet . The hydrogen transfer onto the aromatic ring, also observed for 10^\bullet , can be formulated as intramolecular protonation of the aromatic anion with the ammonium cation. However, the information on the initial proton receptor site is lost in the subsequent fragmentation.

Conclusions

Reduction of substituted benzylammonium cations by collisional electron transfer from organic molecules in the gas phase results in extensive dissociation. Substituents at the ammonium nitrogen and in the aromatic ring affect the dissociations of CH_2-N , $N-H$, and $N-CH_3$ bonds in the transient hypervalent ammonium radicals. Fluorine- and nitro-substituted benzylammonium radicals undergo extensive ring fissions which are attributed to electron capture by the aromatic ring.

Acknowledgment. Support by the National Science Foundation (Grants CHE-9102442 and CHE-9412774), the donors of the Petroleum Research Fund, administered by the American Chemical Society, and the University of Washington Royalty Research Fund is gratefully acknowledged. Computational resources were provided by the Cornell Theory Center, which received major funding from the National Science Foundation and New York state with additional support from the Advanced Research Projects Agency, the National Center for Research Resources at the National Institutes of Health, IBM Corporation, and members of the Corporate Research Institute. We also thank Professor Jurgen Grotemeyer and Dr. Viet Q. Nguyen for helpful discussions.

Supporting Information Available: Tables of neutralization–reionization spectra and HF/3-21G-optimized geometries in a Z-matrix format (6 pages). This material is contained in libraries on microfiche, immediately follows this article in the microfilm version of the journal, and can be ordered from the ACS; see any current masthead page for ordering information.

JO960320U

(43) Birch, A. J.; Hinde, A. L.; Radom, L. *J. Am. Chem. Soc.* **1980**, *102*, 3370.

(44) (a) Trenerry, V. C.; Bowie, J. H. *Org. Mass Spectrom.* **1980**, *15*, 367. (b) Budzikiewicz, H. *Angew. Chem., Int. Ed. Engl.* **1981**, *20*, 624. (c) Stemmler, E. A.; Hites, R. A. *Electron Capture Negative Ion Mass Spectra of Environmental Contaminants and Related Compounds*; VCH Publishers: New York, 1988; p 111.

(40) Smith, D. R.; Raymonda, J. W. *Chem. Phys. Lett.* **1971**, *12*, 269.

(41) Whetten, R. L.; Fu, K.-J.; Tapper, R. S.; Grant, E. R. *J. Phys. Chem.* **1983**, *87*, 1484.

(42) Boesl, U.; Grotemeyer, J.; Muller-Dethlefs, K.; Neusser, H. J.; Selzle, H. L.; Schlag, E. W. *Int. J. Mass Spectrom. Ion Processes* **1992**, *118/119*, 191.